PRESSURE EFFECT ON ATOMIC MOVEMENT IN SUBSTITUTIONAL ALLOYS

by

Edward Daniel Albrecht

A Dissertation Submitted to the Faculty of the

DEPARTMENT OF MINING AND METALLURGICAL ENGINEERING

In Partial Fulfillment of the Requirements
For the Degree of

DOCTOR OF PHILOSOPHY

In the Graduate College

THE UNIVERSITY OF ARIZONA

1 9 6 4

THE UNIVERSITY OF ARIZONA

GRADUATE COLLEGE

I hereby recommend that this dissertation prepared under my direction by **Edward Daniel Albrecht**

entitled **Pressure Effect on Atomic Movement in Substitutional Alloys**

be accepted as fulfilling the dissertation requirement of the degree of **Doctor of Philosophy**

Carl T. Tomizuka — Dissertation Director — April 15, 1964 — Date

After inspection of the dissertation, the following members of the Final Examination Committee concur in its approval and recommend its acceptance:*

Keaton Kelley	April 17, 1964
Kenneth L. Keating	April 17, 1964
Louis J. Demer	April 15, 1964
Daniel J. Murphy	April 16, 1964

*This approval and acceptance is contingent on the candidate's adequate performance and defense of this dissertation at the final oral examination. The inclusion of this sheet bound into the library copy of the dissertation is evidence of satisfactory performance at the final examination.

STATEMENT BY AUTHOR

This dissertation has been submitted in partial fulfillment of requirements for an advanced degree at The University of Arizona and is deposited in the University Library to be made available to borrowers under rules of the Library.

Brief quotations from this dissertation are allowable without special permission, provided that accurate acknowledgment of source is made. Requests for permission for extended quotation from or reproduction of this manuscript in whole or in part may be granted by the head of the major department or the Dean of the Graduate College when in his judgment the proposed use of the material is in the interests of scholarship. In all other instances, however, permission must be obtained from the author.

SIGNED: Edward Daniel Debnath

ACKNOWLEDGMENTS

The author wishes to express his sincere thanks to Professor C. T. Tomizuka for his encouragement and many stimulating discussions concerning this research, to Mr. Rodney C. Lowell for his operation of the high pressure apparatus and advice on high pressure techniques, and to Mr. Robert H. Dickerson for considerable assistance in preparing for this investigation. Special thanks is also extended to Professor T. M. Morris, Professor L. J. Demer, Professor D. J. Murphy and Professor K. L. Keating, all of the Department of Mining and Metallurgical Engineering, for their guidance and advice during his course of study. This project was sponsored in part by the U. S. Atomic Energy Commission through contract AT (11-1)-1041. The support of this agency is gratefully acknowledged.

TABLE OF CONTENTS

LIST OF TABLES

LIST OF FIGURES

ABSTRACT

The diffusion of silver-110 and gold-198 in a nominally gold-34 atomic per cent silver alloy has been measured at 860, 910 and 960 ^{o}C and at hydrostatic pressures from 2070 to 8280 bars. A retarding effect of pressure on the diffusion rate has been observed for both the silver and gold tracers. Temperature determination, uniformity and reproducibility have been found to be the limiting sources of error in pressure-diffusion studies. Activation volumes have been found to be 7.2 cm^3 per mole for silver-110 and 7.5 cm^3 per mole for gold-198. These values are consistent with the theory of Lawson, Rice, Corneliussen and Nachtrieb, and the experimental value of the activation volume of motion of vacancies, ΔV_m, in gold found by Emrick. Changes in activation enthalpy values and frequency factors have been calculated and compared to the experimentally determined values--the agreement is fair. The variation of diffusion rates and activation volumes is explained on the basis of isothermal compressibilities where silver is much more compressible than gold.

I. INTRODUCTION

In recent years, considerable progress has been made in the area of diffusion-controlled phenomena in metal alloys. Phenomena such as anelasticity and tracer diffusion have been studied extensively. In substitutional alloys, investigation of solute diffusion by internal friction and anelastic relaxation have afforded activation energies several Kcal/mole less than those found from direct diffusion studies. This discrepancy is observed when one compares anelastic measurements in silver-zinc alloys by Nowick[1] and diffusion measurements by Lazarus and Tomizuka.[2] A similar discrepancy was found by Hino, Tomizuka and Wert[3] in their study of internal friction and diffusion in an alpha brass containing 31 per cent zinc. These findings indicated a need for further investigation of other substitutional systems.

Tomizuka, Roberts and Dickerson[4] later found an activation energy for self-diffusion of zinc in a silver-15 atomic per cent zinc alloy which was in agreement with the value found by Nowick[1] in his anelastic measurements.

Mallard, Gardner, Bass and Slifkin[5] recently completed an extensive investigation of self-diffusion in the

substitutional gold-silver system in an effort to gain a better understanding of the problem through a high degree of experimental accuracy. Turner and Williams[6] followed with an internal friction and anelastic relaxation experiment for two compositions in this system. The activation energies resulting from these coordinated experiments were essentially in agreement.

Anelastic relaxation experiments in the substitutional silver-30 atomic per cent zinc alloy were performed by Tichelaar and Lazarus[7] in an effort to determine the pressure effect on this diffusion-limited process. They found an exponential increase of relaxation time with increase in pressure.

Self-diffusion measurements have been made under high hydrostatic pressure by Nachtrieb in low-melting-point metals such as lead,[8] sodium[9] and alpha phosphorous[10] and by Tomizuka in silver.[11] The aim of this investigation is to extend the pressure self-diffusion experiment to the substitutional alloy in an effort to gain further information about atomic movement in these materials. The gold-silver system was selected due to the availability of the work of Mallard et al[5] and Turner and Williams.[6]

II. EXPERIMENTAL PROCEDURE

A. Preparation of Material

A single crystal having a nominal composition of gold-34 atomic per cent silver was grown from 99.99% pure gold (Sigmund Cohn) and 99.99% pure silver (Handy and Harmon) in an evacuable, vertical crystal-growing furnace similar to that described by Lazarus and Chipman.[12] Ingots of gold and silver were cast in high-purity graphite crucibles which had been cleaned thoroughly by boiling in aqua regia followed by repeated boiling in distilled water. These ingots were separately prepared by repeated degassing at 1200°C and combined and recast three times in vacua of 6×10^{-6} mm of mercury, the ingot being inverted after each cycle to insure homogeneity. The cooling rate for single crystal growth was 20°C per hour. (See Appendix I for further description of the apparatus.)

Cylindrical specimens 0.410 inch in diameter and $\frac{1}{4}$ inch thick were sawed from the single crystal bar. The usual metallographic procedure was employed to cut, polish and anneal the specimens.

The composition of each specimen was determined by the liquid-displacement method using bromobenzene as the

liquid. A linear relationship between density and concentration was assumed.[5] Composition was found to vary from 66.0 to 66.4 atomic per cent gold between specimens.

Gold-198 followed by silver-110, obtained from the Oak Ridge National Laboratory, were electroplated from weak acid solutions onto each specimen thereby allowing subsequent simultaneous diffusion of two radioisotopes under identical conditions. The plated layer was calculated to be less than 1000 angstroms in total thickness. (The electroplating and radioisotope-handling facility is shown in Appendix II.)

B. Apparatus

A gas pressure system similar to that of Goldsmith and Heard[13] was used. The pressure medium was composed of argon with from 5 to 20% helium. Helium was added to permit the use of a helium leak detector to locate leaks in the pressure system.

The working volume within the experimental chamber under high pressure was limited to 1 inch diameter by $6\frac{1}{2}$ inches in length. This space limitation created many experimental difficulties related to the operation of the high-temperature furnace, such as temperature uniformity and measurement.

An internal, high-temperature furnace was made from a threaded lavite core, closely wound with 0.016-inch diameter platinum wire and contained in a lavite sheath. The specimen and thermocouple were placed in intimate contact within a lavite specimen holder which filled the furnace core, thereby reducing the free volume within the pressure vessel. Power and thermocouple leads were brought from the vessel via steel, chromel and alumel cones electrically insulated from the apparatus plug by lavite as described by Bridgman[14] and Emrick.[15] The high-pressure side of the plug was coated with Eccobond 76 epoxy to fill the shallow gap between plug and cone which was created when the lavite insulator was excessively extruded and crumbled at this surface during assembly. Electrical arcing encountered frequently before the use of the epoxy was practically eliminated after the coating was applied. (See Appendix III for details of the high-pressure system and internal furnace.)

Chromel-alumel thermocouples were used because of the small change in emf due to elevated pressure as reported by Bundy.[16] It was found that thermocouples used in their usual configuration were extremely variable in their calibration after use at high temperatures and pressures for periods of several hours. These variations followed no observable trend with time, temperature or pressure and were sometimes

positive and other times negative. Several thermocouple configurations were developed and tested and the final experimental thermocouple was composed of a flat 0.003-inch thick platinum disk 0.375 inch in diameter with unoxidized B and S No. 24 chromel and alumel wires spot-welded to the disk which acted as the thermocouple bead. A new thermocouple was used with each specimen and each was calibrated after use against a standard platinum-platinum 10% rhodium thermocouple which had been previously calibrated with NBS standard melting point metals. Final calibrations again proved to be irregular, but to a much lesser degree than observed in preliminary tests. Calibrations of the experimental thermocouples were not made before actual use for reasons discussed later in this paper. (The calibration furnace is shown in Appendix II.)

Temperature was controlled to ± 0.5°C during the diffusion anneals. Warm-up corrections were made to the diffusion times to account for the approximately five-minute time from room temperature to annealing temperature and the quench time of three minutes or less to room temperature. The corrected annealing times for all specimens were from 150 to 152 minutes. (The temperature-controlling apparatus is shown in Appendix II.)

Pressure was maintained constant, to within ± 10 bars, during warm-up, the diffusion anneal and until 600°C was reached during the quench. The pressure was measured with a manganin pressure gauge calibrated at the freezing pressure (7640 bars) of mercury at 0°C.

Standard lathe sectioning and weighing techniques described by Tomizuka[17] were employed after the diffusion anneals. Sections of thickness ranging from 0.0003 to 0.0005 inch were removed from each specimen. (The equipment used is shown in Appendix II.)

The gamma activity of the lathe sections was counted by a scintillation counter and an RIDL model 34-12B, 400 channel analyzer. In order to separate the gamma peaks of the silver-110 from those of the gold-198, preliminary measurements were made to subtract the background of one isotope from the peak of the other. This was accomplished by determining the ratio, at several activities, of silver-110 counts at 0.656 Mev to the silver-110 background at the 0.411 Mev level where the gold-198 peak would appear. The gold-198 contributed no measurable background to the silver-110 peak and permitted the silver-110 to be left uncorrected. A predetermined percentage of the count at the silver-110 peak was subtracted from the gold-198 peak to gain the final value of activity due to this isotope. The live-time

counting mode was employed for all counts and thereby automatically corrected for the dead-time of the analyzer. (The counting apparatus is shown in Appendix II.)

III. EXPERIMENTAL RESULTS

Twelve pressure-diffusion anneals were made resulting in twelve diffusion coefficients for each tracer in the nominally 66 atomic per cent gold alloy. The temperature range from 860 to 960°C was investigated at pressures from 2070 to 8280 bars. Figures 1 through 4 show that the specific activity of the lathe sections decreases exponentially as the square of the penetration depth. Diffusion coefficients derived from the penetration curves, temperatures, pressures and times of diffusion anneals are tabulated in Table I.

IV. DISCUSSION

A. Treatment of the Data

The diffusion coefficients, D, were obtained from the slopes of the penetration plots. Figure 5 shows data plotted as the common logarithm of diffusion coefficient versus the reciprocal of absolute temperature. The straight lines that best fit the data for the 2070, 4140 and 8280 bar isobars and a corrected line for the 6210 bar isobar are given by the following equations:

$$D_{Ag}^{2070} = 0.025 \exp(-38{,}400/RT)$$

$$D_{Ag}^{4140} = 0.053 \exp(-40{,}500/RT)$$

$$D_{Ag}^{6210} = 0.24 \exp(-44{,}500/RT)$$

$$D_{Ag}^{8280} = 0.86 \exp(-48{,}000/RT)$$

$$D_{Au}^{2070} = 0.018 \exp(-39{,}200/RT)$$

$$D_{Au}^{4140} = 0.050 \exp(-42{,}100/RT)$$

$$D_{Au}^{6210} = 0.22 \exp(-46{,}000/RT)$$

$$D_{Au}^{8280} = 1.7 \exp(-51{,}300/RT)$$

where the subscripts on D represent the solute tracer and the superscripts on D represent the pressure in bars. (Details of the solution of the diffusion equation are given in Appendix IV.)

Calculations were made for the variation of activation enthalpy, H_p, with pressure on the basis of the relation,

$$H_p = H_o + (\partial H/\partial P)_T \, \Delta P.$$

Ignoring the entropy term, one can approximate the above relation by

$$H_p \cong H_o + \Delta V \Delta P$$

where the quantities on the right are known, the H_o being extracted from the work of Mallard et al,[5] and ΔV being the activation volume discussed later in this paper. The calculated and experimental values of H_p were found to be in fair agreement as shown in Table II.

The frequency factor, D_o, from the Arrhenius-type equation

$$D = D_o \exp(-H_p/RT)$$

was calculated from the experimental D and H_p as well as the calculated H_p for the particular pressures involved and the resulting pressure dependency recorded in Table II.

The results of pressure diffusion experiments are conveniently summarized in terms of an activation volume, ΔV, which for the diffusion process is considered to be a measure of the volume relaxation around a vacancy and is related to the volume of a mole of vacancies in motion. Plots of the common logarithm of diffusion coefficient versus pressure for silver and gold tracers are given in Figures 6 and 7, where the lines were obtained by a least-squares analysis.

Activation volume is expressed in terms of the Gibbs free energy, ΔG, as

$$\Delta V = (\partial \Delta G/\partial P)_T$$

where ΔV is composed of ΔV_f, the volume of formation of a vacancy, and ΔV_m, the volume of motion of a vacancy. It then follows that[18]

$$\Delta V = -RT(\partial \ \ell n \ D/\partial P)_T - RT(\partial \ \ell n \ \gamma a^2 \overline{\nu} f/\partial P)_T$$

where R is the gas constant, γ is the geometrical factor, of the order of unity for f.c.c. crystals, a is the lattice parameter, $\overline{\nu}$ is the vibrational frequency, f is the correlation factor, and all other terms have their usual meaning.

The magnitude of the second term was estimated and found to be less than 2% of the total contribution to ΔV in this specific investigation and is therefore neglected in the calculations. The effect of the correlation factor, f, was ignored. From the ΔV values given in Table III, one can calculate a value for $\Delta V/\Delta V_M$ of 73% for gold and 70% for silver, where ΔV_M is the molar volume.

Pressure-diffusion experiments measure an actual volume change in a finite specimen. According to Eshelby,[19] the local relaxation about a center of dilation or compression will produce a greater relaxation in the volume of the entire solid because of the image term arising from the free surface. Considering an isotropic solid, he has shown that the measured ΔV is greater than the local relaxation by a factor of $3(1 - \sigma)/(1 + \sigma)$ where σ is Poisson's ratio. Estimating a Poisson's ratio for this alloy to be 0.392, this factor is 1.53 which yields an unrelaxed defect volume of 4.7 cm^3/mole for silver and 4.9 cm^3/mole for gold.

B. Discussion of Errors

The limiting source of error in this experiment was temperature measurement and its reproducibility. Some scatter occurred, as expected, in the 960°C data due to temperature measuring difficulties. However, the greatest errors were encountered at 860°C where initially the sources of error were considered to be smallest. Data obtained from the 910°C diffusions have been taken as the most valid, because all preliminary tests, procedures and equipment designs were made for this temperature.

Thermocouples made from the same spools of wire were calibrated against the standard thermocouple and compared to the experimental thermocouple configuration. Additive errors of $1\frac{1}{2}$ to 2°C were found for each successive heat-up to temperatures in the region of the diffusion-anneal temperature. For this reason thermocouples were not calibrated before the anneal. A calibration described earlier was performed after the anneal and the final value of temperature was established on the basis of the initial wire calibration, error due to second heat-up for final calibration and one-half the temperature correction due to high temperature and pressure deterioration during the diffusion anneal. It was assumed that the deterioration was linear

and that the value of one-half would yield an average temperature of the anneal. The source of error has been attributed to some uncontrollable contamination from the gas pressure medium or vessel parts which are not effective at atmospheric pressure.

The diffusion anneals were purposely randomized with reference to pressure and temperature to minimize creation of trends in the data due to composition changes in the gas mixture, varying characteristics of the internal furnace and varying leak rates due to wearing of the seals in the pressure system.

C. Discussion of the Results

Theoretical calculation of ΔV_f has been attempted by Lawson, Rice, Corneliussen and Nachtrieb.[20] Their results show that ΔV_f can be expressed in terms of the Grüneisen constant, γ_G, where

$$\Delta V_f / \Delta V_M = (\gamma_G - 2/3)^{-1}$$

and ΔV_M is the molar volume. Tewordt[21] has considered the relaxation around a vacancy specifically for copper and his calculation yielded a value of 0.47 to 0.55 molar volume for ΔV_f. An experimental value for the ΔV_f in gold has been

determined to be 0.53 ± 0.04 molar volume by Huebener and Homan.[22] A value for ΔV_m for gold has been found by Emrick,[14] in his studies of the annealing rate of quenched-in vacancies, to be 0.15 ± 0.014 molar volume. In the present work both gold-198 and silver-110 were diffused simultaneously in the same specimen so that all conditions of temperature, pressure and annealing time were identical for both isotopes. For this reason, the difference between the activation volume for gold and that for silver is considerably more significant and reliable than the absolute values of ΔV. The difference in ΔV, if significant, must be attributed to a difference in ΔV_m since ΔV_f for a vacancy does not vary from one site to another in a random substitutional alloy where both constituents are present in comparable percentages. Assuming a value of 55% for ΔV_f, for either isotope, which agrees with the theory, one gets 73 - 55 = 18% for ΔV_m for gold-198 and 70 - 55 = 15% for silver-110.

Although atomic diameters of gold and silver are nearly equal, as are their nominal valences, there are considerable differences in their isothermal compressibilities, with silver being much more compressible than gold.[23] The less compressible closed shell of gold requires more energy and more volume expansion to pass through the saddle point configuration than silver. Even though the compressibilities

of the individual gold and silver ions are expected to be different from those in their respective pure matrices they nevertheless indicate the relative deformability of ions at the saddle point configuration.

The temperature dependence of ΔV observed in this investigation is attributed, in the most part, to experimental error and should not be considered as significant.

The three points per line in the plot of common logarithm of diffusion coefficient versus the reciprocal of absolute temperature, Figure 5, are insufficient to yield definitive activation enthalpy values. However, there are observable trends which agree with the predictions from the calculated H_p and D_o.

From this investigation it can be seen readily that a great deal of further work is needed in this area. More reliable and predictable methods of temperature determination are of utmost importance before more accurate pressure diffusion data can be obtained. Once this is realized, several more temperatures should be considered for the gold-34 atomic per cent silver alloy in order to allow for better determination of H_p and D_o. A study of anelastic relaxation similar to the work of Tichelaar and Lazarus[7] should be made to complement the present work. A quenching and annealing of vacancies experiment, in this alloy, as performed by

Emrick,[14] would yield an independent experimental value for ΔV_m. Some of these investigations are presently under way in this laboratory.

V. CONCLUSIONS

The conclusions reached as a result of this investigation are as follows:

1. Self-diffusion in the substitutional, nominally gold-34 atomic per cent silver alloy has a marked pressure dependence.

2. The average activation volumes of 73% for the slower-diffusing gold and 70% for the faster-diffusing silver are in good agreement with existing theories.

3. The differences in the diffusion rates and activation volumes for gold and silver can be explained on the basis of their isothermal compressibilities.

TABLE I

Diffusion Coefficients for gold and silver tracers

Run No.	Composition Atomic % Gold	Pressure bars	Temperature °C	Diffusion Coefficient in cm^2/sec Silver-110	Gold-198
15	66.3	2070	856	1.04×10^{-9}	5.21×10^{-10}
14	66.4	4140	857	7.38×10^{-10}	3.99×10^{-10}
11	66.1	6210	857	7.32×10^{-10}	3.51×10^{-10}
8	66.3	8280	858	4.25×10^{-10}	2.08×10^{-10}
4	66.2	2070	911	1.85×10^{-9}	9.07×10^{-10}
9	66.0	4140	914	1.75×10^{-9}	8.44×10^{-10}
5	66.3	6210	907	1.30×10^{-9}	6.25×10^{-10}
6	66.1	8280	909	1.07×10^{-9}	5.31×10^{-10}
13	66.3	2070	963	4.61×10^{-9}	2.31×10^{-10}
12	66.1	4140	962	3.84×10^{-9}	1.91×10^{-10}
10	66.4	6210	961	2.74×10^{-9}	1.33×10^{-10}
7	66.2	8280	960	2.86×10^{-9}	1.43×10^{-10}

TABLE II

Activation enthalpy, H_p and frequency factor, D_o, for gold and silver tracers

Tracer	Pressure bars	Calculated H_p cal./mole	Calculated D_o	Experimental H_p cal./mole	Experimental D_o
Silver	2070	42,100	0.12	38,400	0.025
Silver	4140	42,400	0.12	40,500	0.053
Silver	6210	42,800	0.11	44,500	0.24
Silver	8280	43,100	0.11	48,000	0.86
Gold	2070	44,900	0.20	39,200	0.018
Gold	4140	45,200	0.19	42,100	0.050
Gold	6210	45,600	0.18	46,000	0.22
Gold	8280	46,000	0.18	51,300	1.7

TABLE III

Activation volumes for diffusion of gold and silver tracers

Tracer	Temperature °C	ΔV $cm^3/mole$	ΔV (average) $cm^3/mole$
Silver	860	8.3	
Silver	910	7.2	7.2
Silver	960	6.1	
Gold	860	8.3	
Gold	910	7.4	7.5
Gold	960	6.9	

Figure 1. Penetration curve for diffusion of gold and silver in gold-34 atomic per cent silver alloy at 2070 bars.

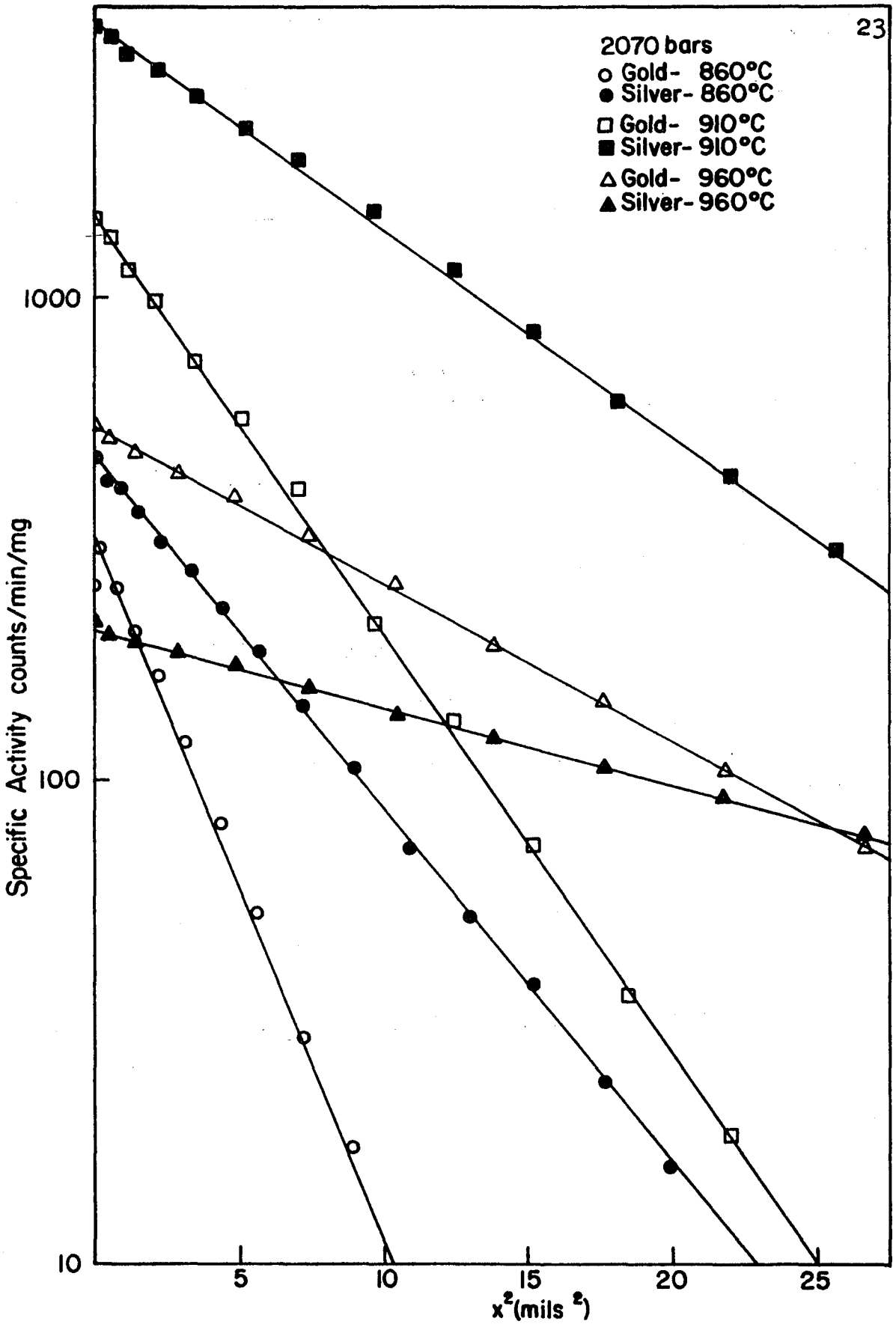
2070 bars
Gold- 860°C
Silver- 860°C
Gold- 910°C
Silver- 910°C
Gold- 960°C
Silver- 960°C
Specific Activity counts/min/mg
1000
100
10
5
10
15
20
25
x² (mils²)

Figure 1.

Figure 2. Penetration curve for diffusion of gold and silver in gold-34 atomic per cent silver alloy at 4140 bars.

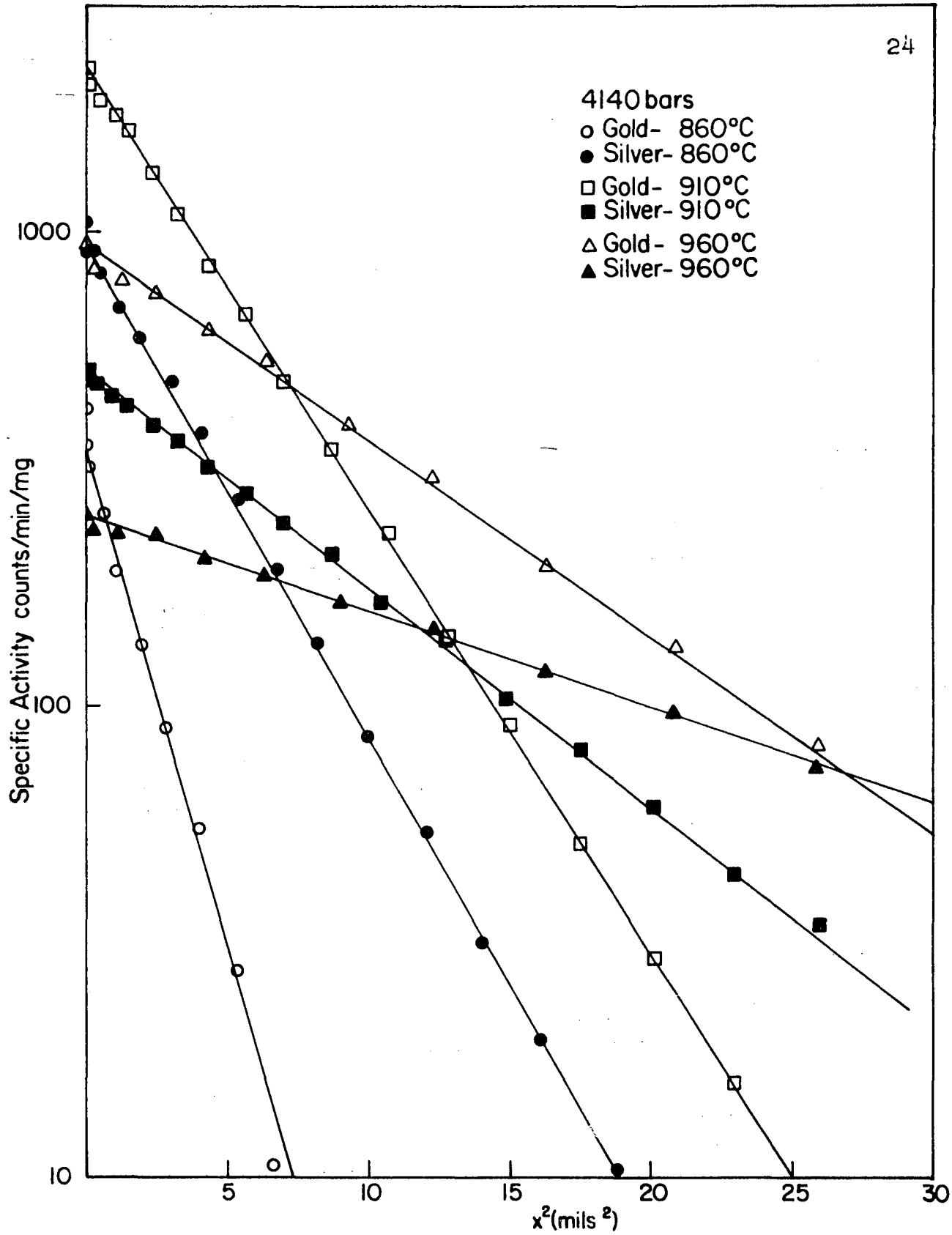
4140 bars
o Gold- 860°C
● Silver- 860°C
□ Gold- 910°C
■ Silver- 910°C
△ Gold- 960°C
▲ Silver- 960°C
Specific Activity counts/min/mg
1000
100
10
5
10
15
20
25
30
x² (mils²)

Figure 2.

Figure 3. Penetration curve for diffusion of gold and silver in gold-34 atomic per cent silver alloy at 6210 bars.

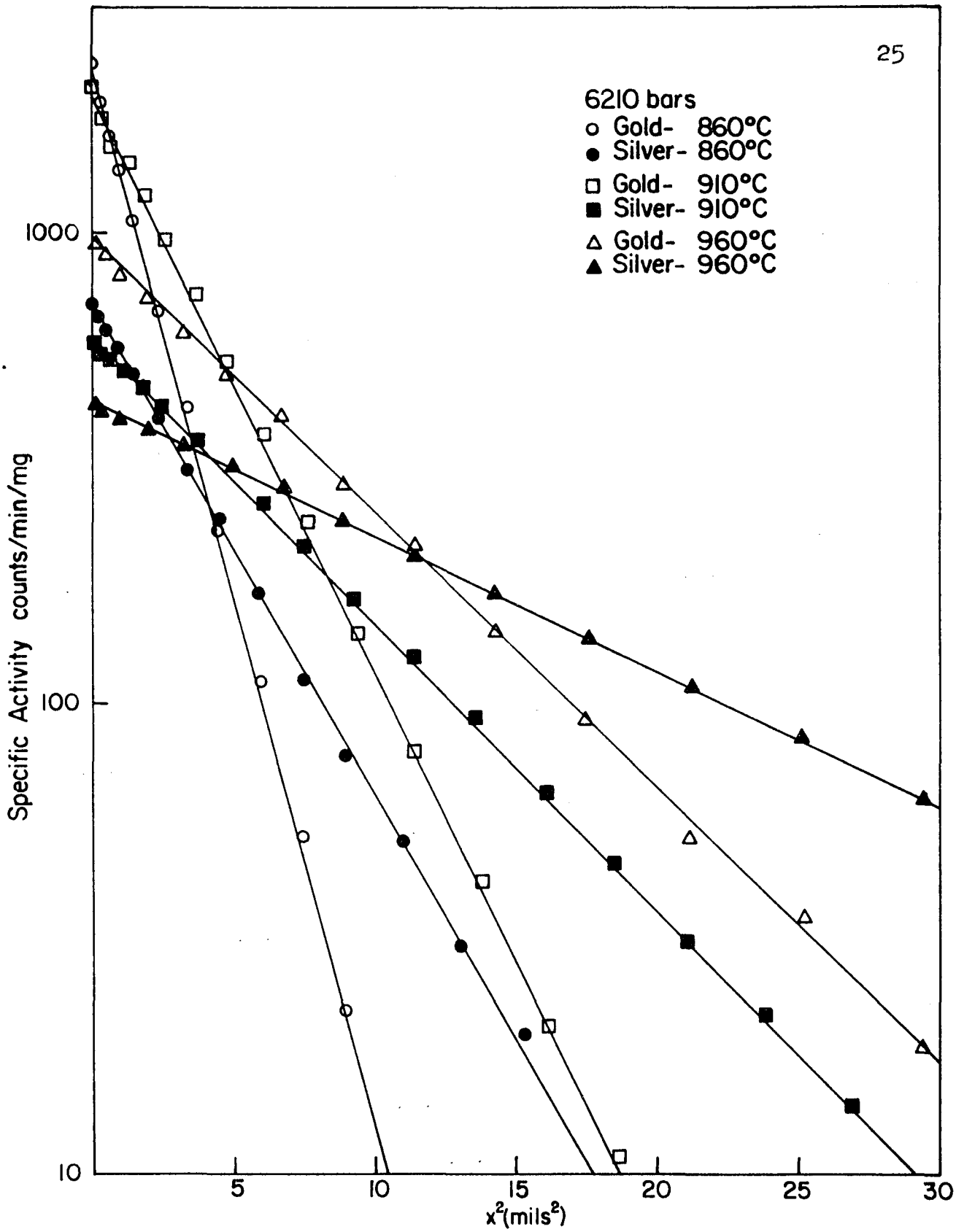
25
6210 bars
Gold- 860°C
Silver- 860°C
Gold- 910°C
Silver- 910°C
Gold- 960°C
Silver- 960°C
1000
100
10
Specific Activity counts/min/mg
5
10
15
20
25
30
x²(mils²)

Figure 3.

Figure 4. Penetration curve for diffusion of gold and silver in gold-34 atomic per cent silver alloy at 8280 bars.

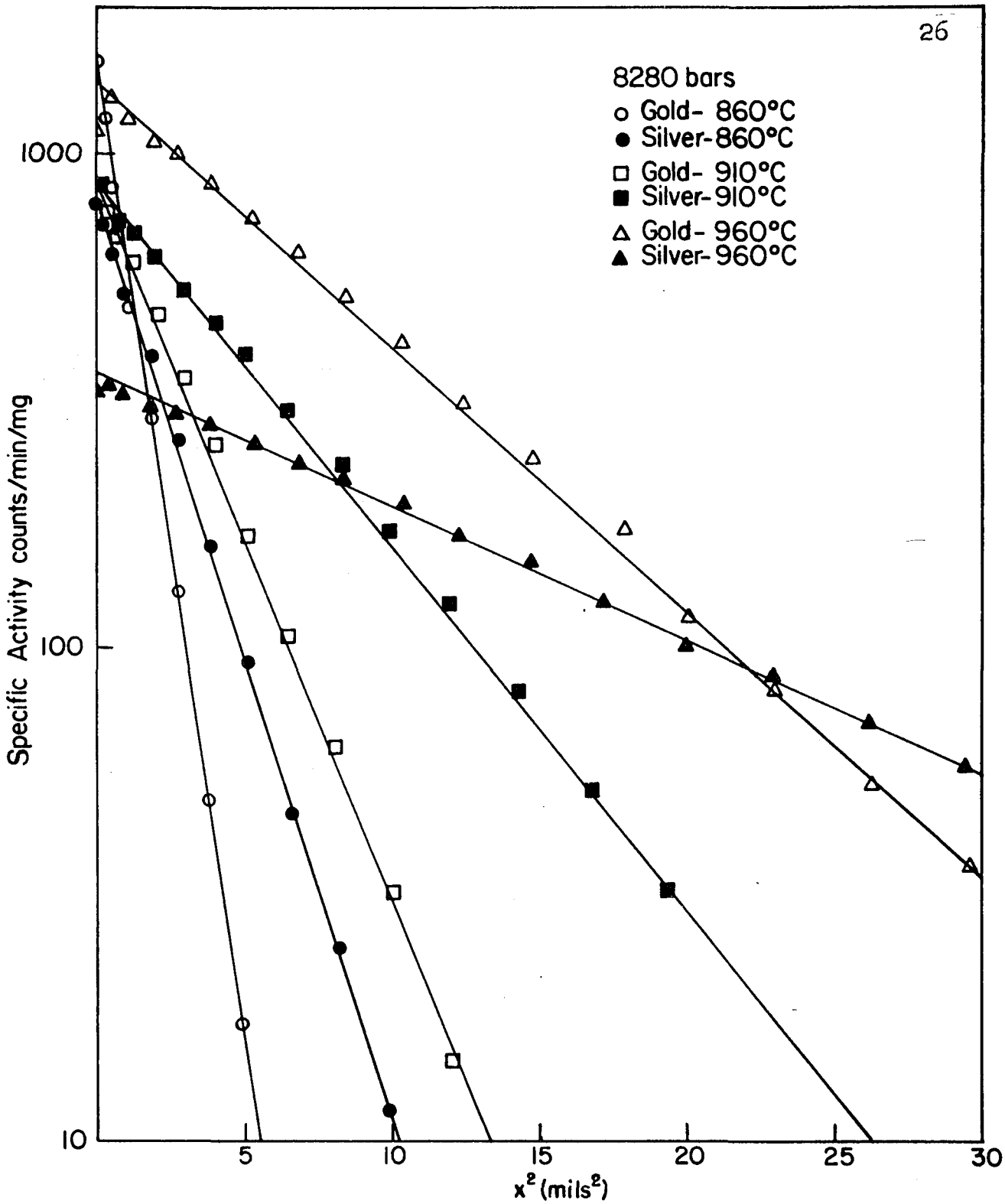
8280 bars
Gold- 860°C
Silver-860°C
Gold- 910°C
Silver-910°C
Gold- 960°C
Silver-960°C
1000
100
10
Specific Activity counts/min/mg
5
10
15
20
25
30
x² (mils²)

Figure 4.

Figure 5. Diffusion data plotted as log D versus 1/T isobars.

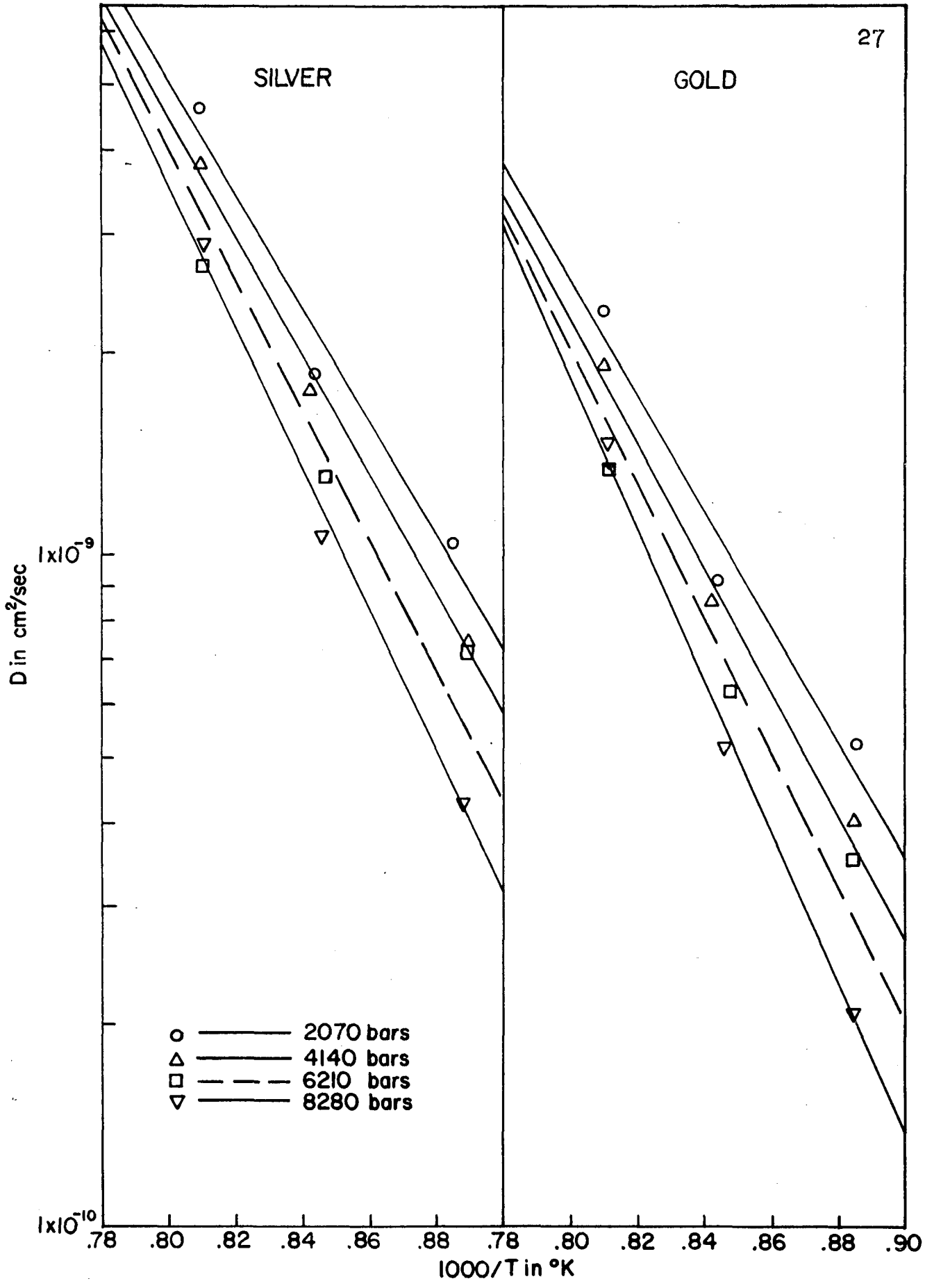
SILVER
GOLD
D in cm²/sec
1x10⁻⁹
1x10⁻¹⁰
2070 bars
4140 bars
6210 bars
8280 bars
.78
.80
.82
.84
.86
.88
.90
1000/T in °K

Figure 5.

Figure 6. Variation with pressure of the gold self-diffusion coefficient in gold-34 atomic per cent silver alloy.

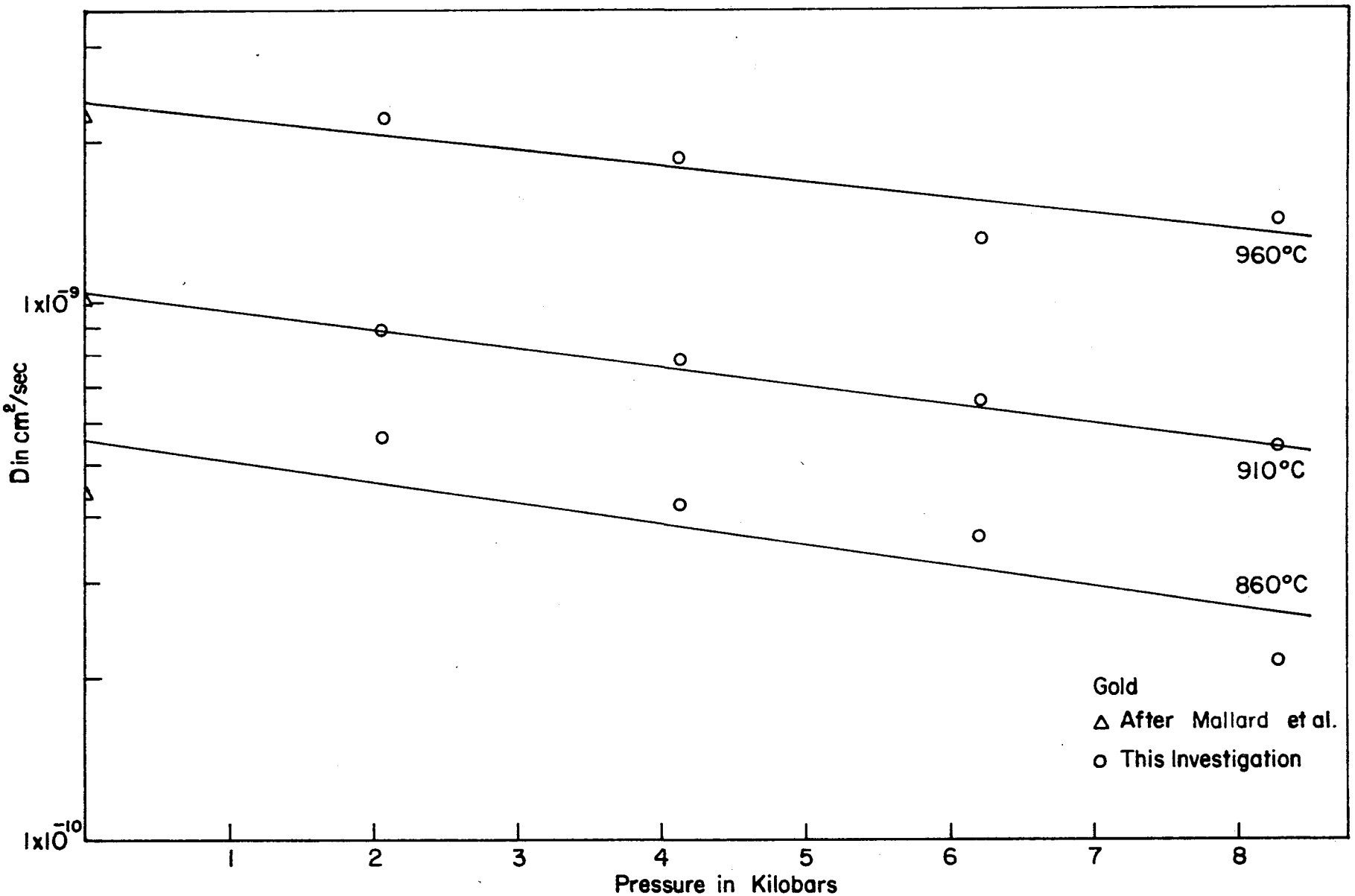
960°C
910°C
860°C
1x10⁻⁹
1x10⁻¹⁰
D in cm²/sec
1
2
3
4
5
6
7
8
Pressure in Kilobars
Gold
△ After Mallard et al.
o This Investigation

Figure 6.

Figure 7. Variation with pressure of the silver self-diffusion coefficient in gold-34 atomic per cent silver alloy.

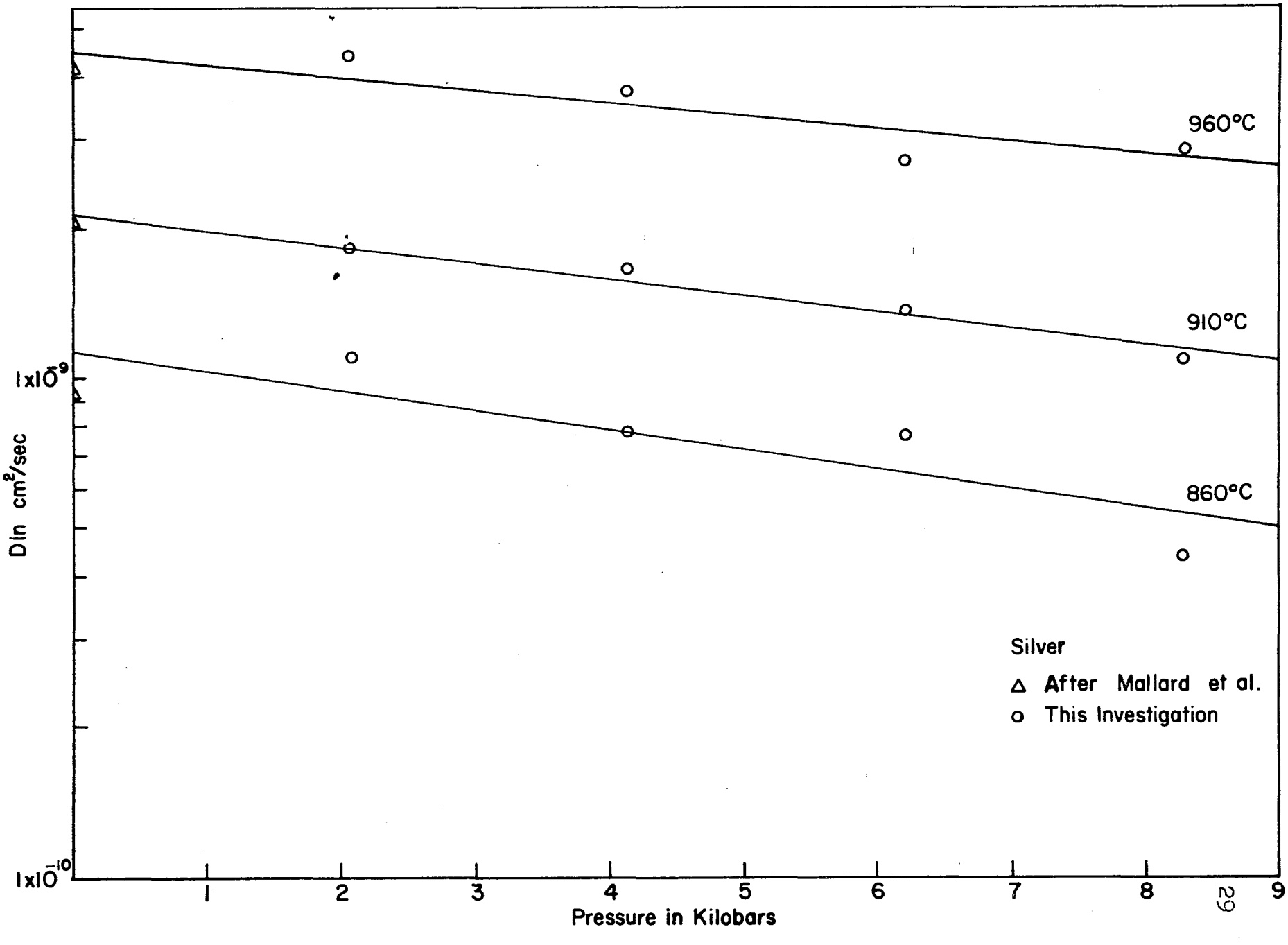
960°C
910°C
860°C
1x10⁻⁹
1x10⁻¹⁰
Din cm²/sec
1
2
3
4
5
6
7
8
9
Pressure in Kilobars
Silver
△ After Mallard et al.
o This Investigation

Figure 7.

LIST OF REFERENCES

1. A. S. Nowick, Phys. Rev. 79, 601 (1952).
2. D. Lazarus and C. Tomizuka, Phys. Rev. 103, 1155 (1956).
3. J. Hino, C. Tomizuka and C. Wert, Acta Met. 5, 41 (1957).
4. C. Tomizuka, R. Roberts and R. Dickerson, Bull. Amer. Phys. Soc. 6, 172 (1961).
5. W. C. Mallard, A. B. Gardner, R. F. Bass and L. M. Slifkin, Phys. Rev. 129, 617 (1963).
6. T. J. Turner and G. P. Williams, Acta Met. 10, 305 (1962).
7. G. W. Tichelaar and D. Lazarus, Phys. Rev. 113, 438 (1959).
8. N. H. Nachtrieb, H. A. Resing and S. A. Rice, J. Chem. Phys. 31, 135 (1959).
9. N. H. Nachtrieb, J. A. Weil, E. Catalano and A. W. Lawson, J. Chem. Phys. 20, 1189 (1952).
10. N. H. Nachtrieb and A. W. Lawson, J. Chem. Phys. 23, 1193 (1955).
11. C. T. Tomizuka, in Progress in Very High Pressure Research edited by F. P. Bundy, W. R. Hibbard, Jr. and H. M. Strong (John Wiley and Sons Inc., New York, 1961).
12. D. Lazarus and D. R. Chipman, Rev. Sci. Inst. 22, 211 (1951).
13. J. R. Goldsmith and H. C. Heard, J. of Geol. 69, 45 (1961).
14. P. W. Bridgman, The Physics of High Pressure, (G. Bell and Sons, Ltd., London, 1958), p. 52.
15. R. M. Emrick, Phys. Rev. 122, 1720 (1961).

16. F. P. Bundy, in Progress in Very High Pressure Research edited by F. P. Bundy, W. R. Hibbard, Jr. and H. M. Strong (John Wiley and Sons Inc., New York, 1961).

17. C. T. Tomizuka, in Methods in Experimental Physics, edited by K. Lark-Horovitz and V. A. Johnson (Academic Press Inc., New York, 1959), Vol. 6.

18. N. H. Nachtrieb, Wright Air Development Center Technical Report 55-68 (1954), p. 32.

19. J. D. Eshelby, J. Appl. Phys. 25, 255 (1954).

20. A. W. Lawson, S. A. Rice, R. D. Corneliussen and N. H. Nachtrieb, J. Chem. Phys. 32, 447 (1960).

21. L. Tewordt, Phys. Rev. 109, 61 (1958).

22. R. P. Huebener and C. G. Homan, Phys. Rev. 129, 1162 (1963).

23. C. Kittel, Introduction to Solid State Physics, (John Wiley and Sons, Inc., New York, 1960), p. 99.

APPENDIX I

Crystal-Growing Furnace

A cross-sectional view of the evacuable crystal-growing furnace is shown in Figure 8 and the actual apparatus is shown in Figure 9. The three O-ring vacuum seals are shown at the top and bottom of the mullite furnace-tube and have been used to attain pressures of 8×10^{-7} mm of mercury at room temperature as measured by a CVC type G1C-110 ionization gauge. Heat is extracted from the graphite crucible by water cooling the bottom end of a 5/8 inch diameter copper rod which is threaded into a medium carbon steel pedestal in intimate contact with the graphite crucible. Steel was used for the pedestal material due to the high melting temperatures of the metals to be cast. The graphite mold was designed with a 3/8 inch long by 3/32 inch diameter seed tip to allow one crystal to become predominant if more than one crystal began growth, before the final 3/8 to 5/8 inch diameter was reached. This design has proven to be exceptionally effective in the growth of copper, gold, silver and gold-silver alloy crystals of various diameters. The quality of the surface finish of the crucible walls has proven to be the limiting factor in successful single crystal growth.

Figure 8. Cross-sectional diagram of crystal-growing furnace.

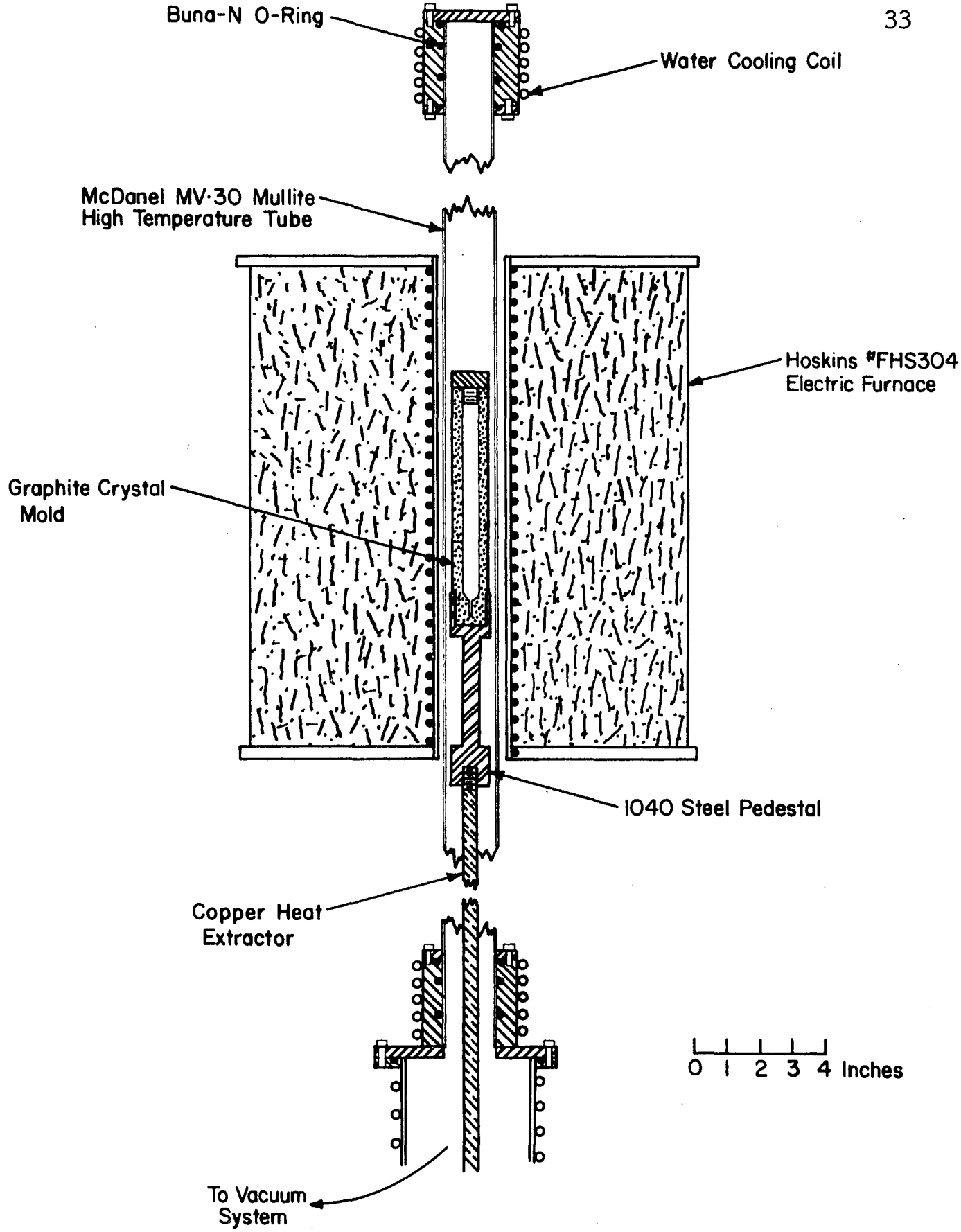
Buna-N O-Ring
Water Cooling Coil
McDanel MV-30 Mullite
High Temperature Tube
Hoskins #FHS304
Electric Furnace
Graphite Crystal
Mold
1040 Steel Pedestal
Copper Heat
Extractor
0 1 2 3 4 Inches
To Vacuum
System

Figure 8.

Figure 9. Crystal-growing furnace and vacuum system.

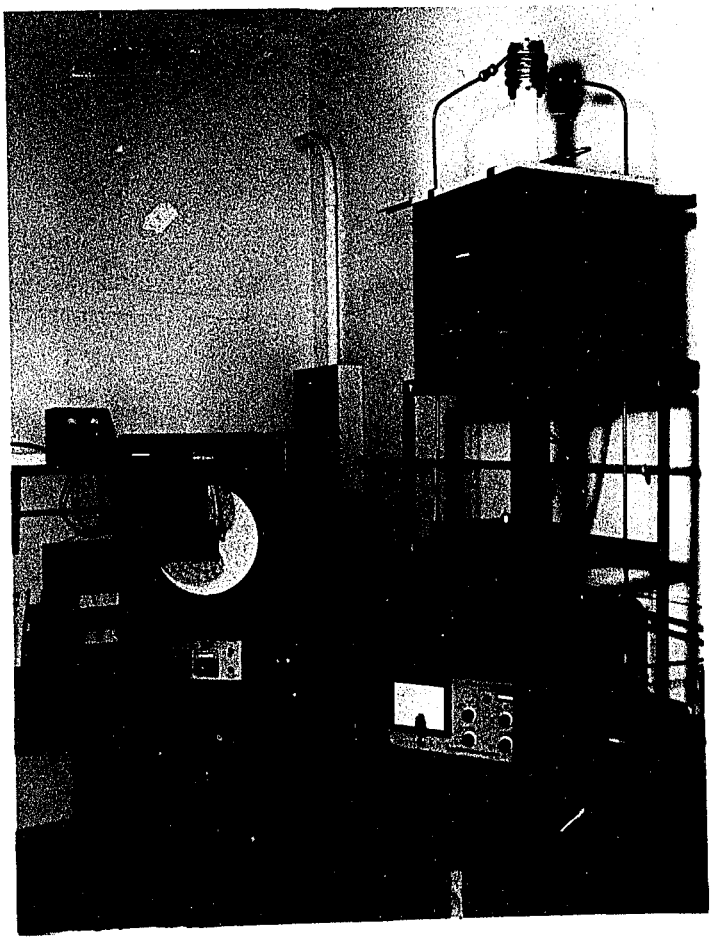

Figure 9

APPENDIX II

Equipment Photographs

Photographs of several pieces of equipment pertinent to this investigation are shown here in an attempt to illustrate the description given in the text.

Figure 10. Electroplating and radioisotope handling facility.

Figure 11. Thermocouple calibration furnace.

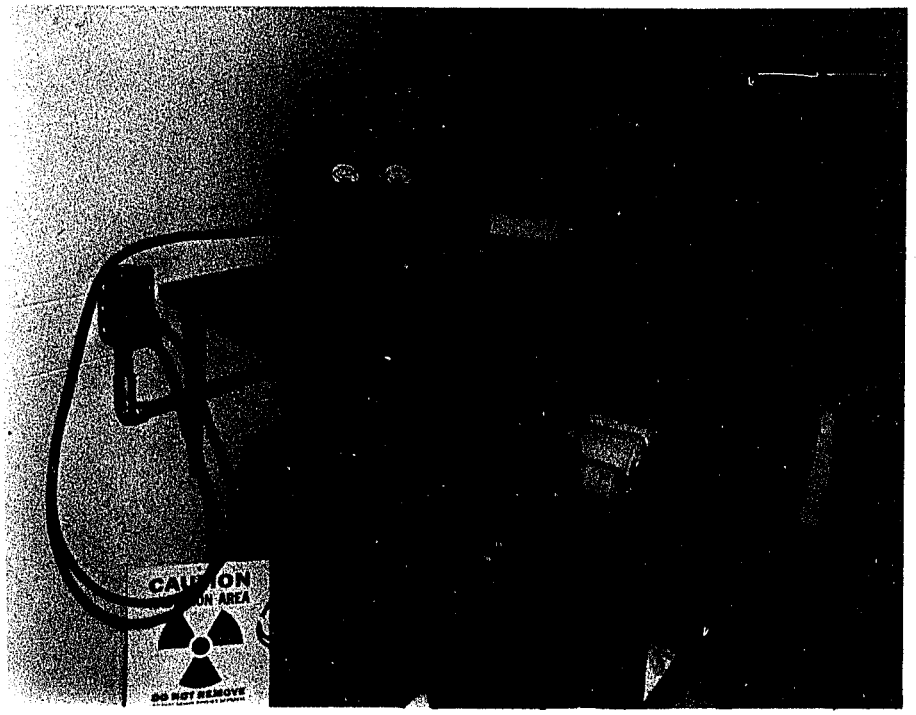

Figure 10

Figure 11

Figure 12. Variable transformer and slide-wire resistor temperature control system.

Figure 13. Mettler precision balance.

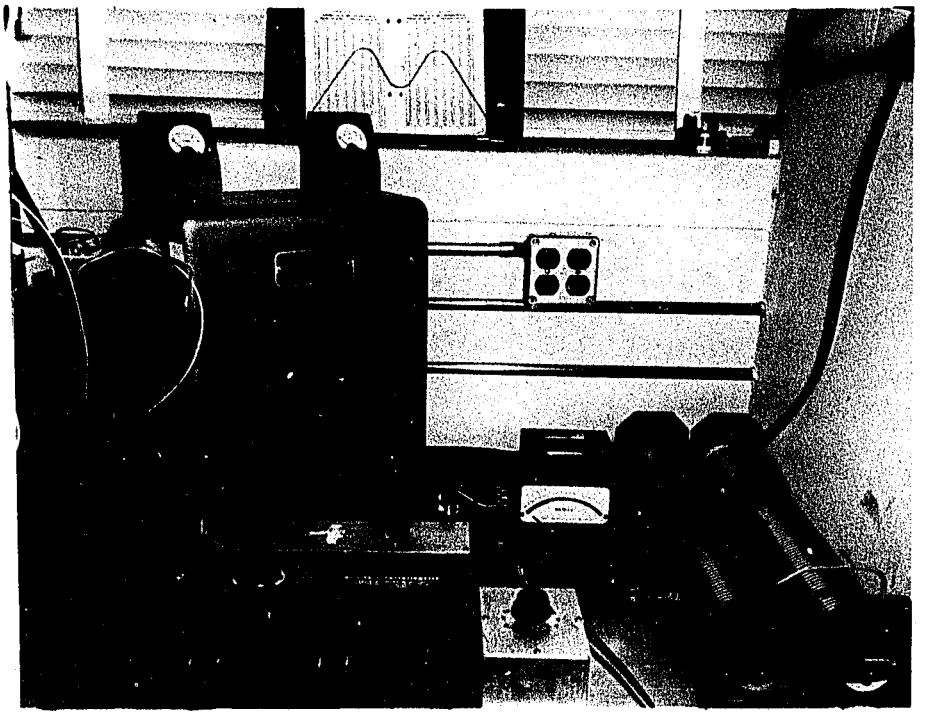

Figure 12

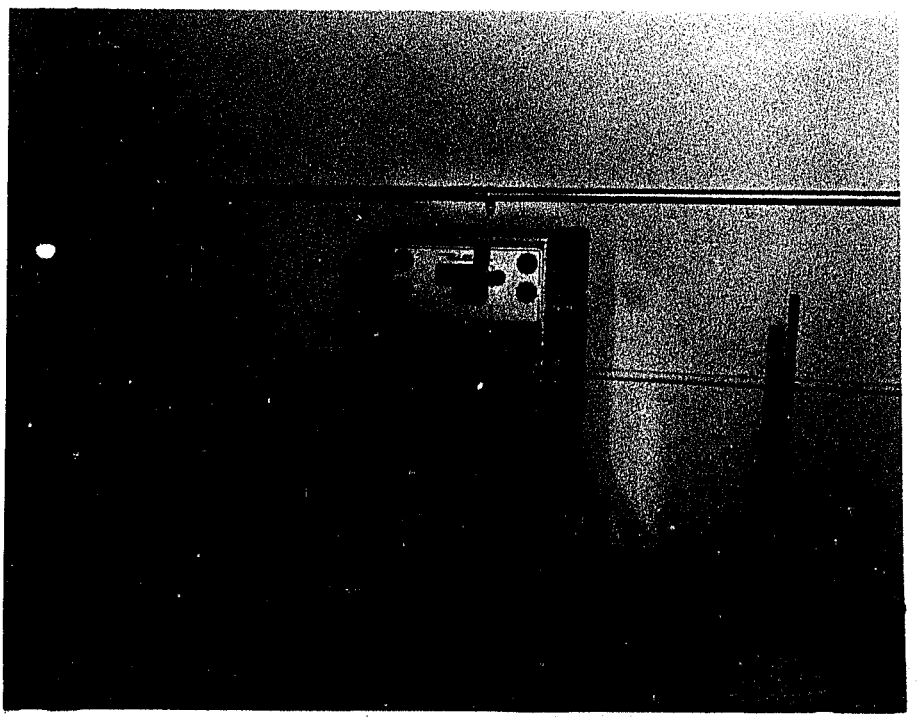

Figure 13

Figure 14. Precision lathe.

Figure 15. Close-up of adjustable chuck and sectioning tool used on the precision lathe.

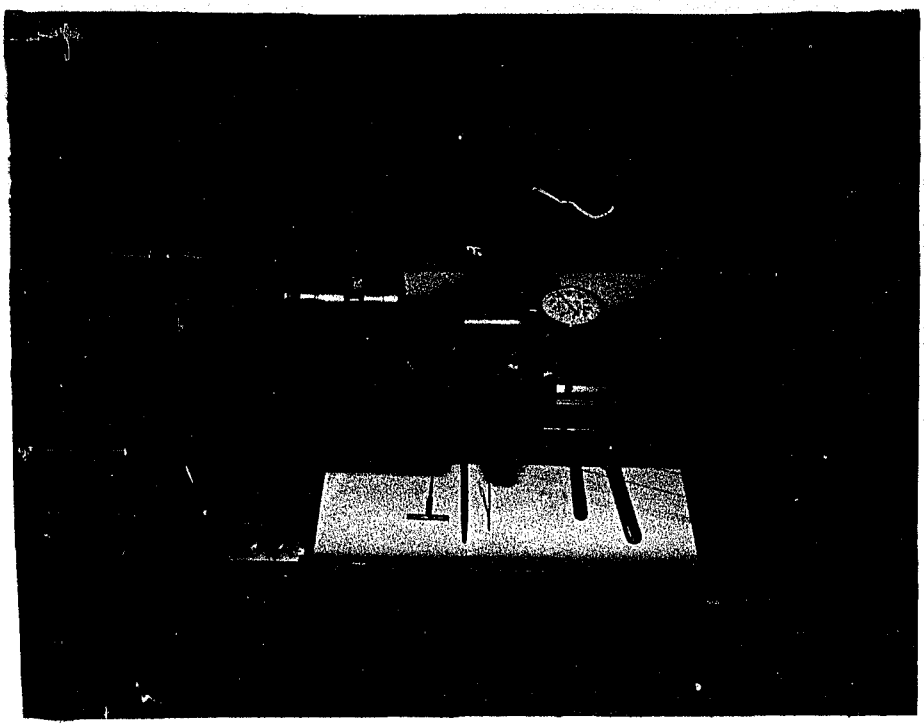

Figure 14

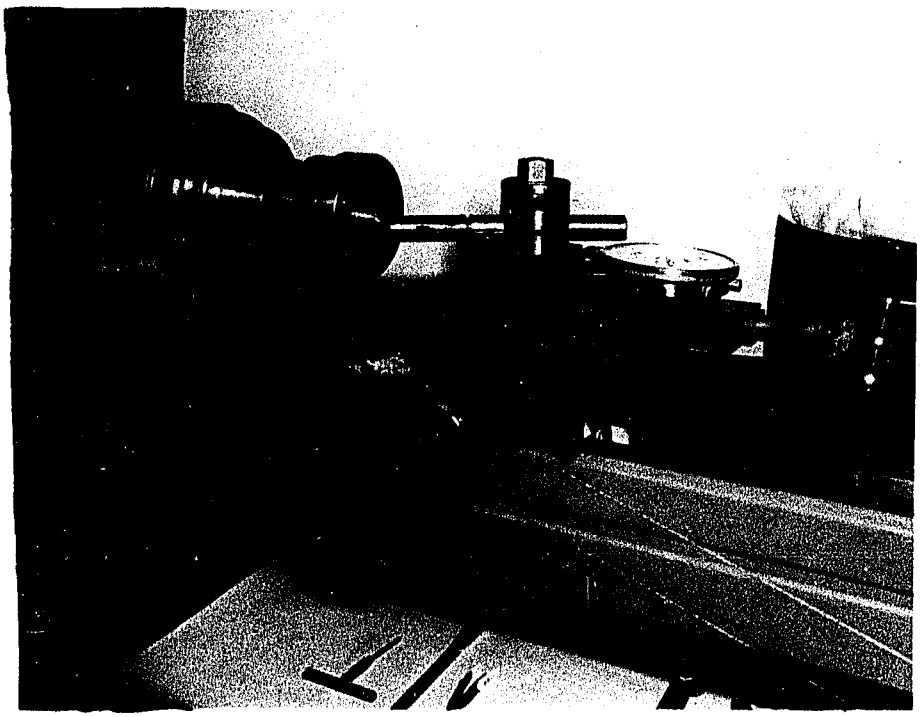

Figure 15

Figure 16. RIDL 400 channel analyzer.

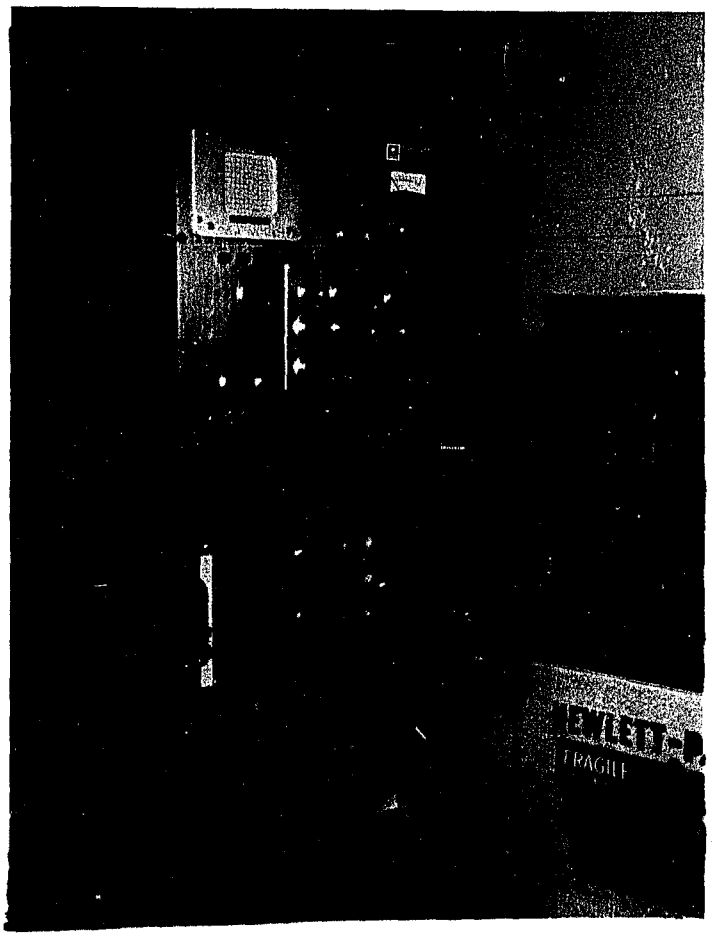

Figure 16

APPENDIX III

Gas Pressure-System and Internal Furnace

A schematic drawing of the hydrostatic, gas pressure-system is given in Figure 17. Photographs of the system and controls are shown in Figures 18 and 19. Pressures to 8280 bars, for this investigation, were generated from an argon-helium tank pressure of about 170 bars and piped to the experimental vessel in two stages. The primary gas-compression stage was produced by a separator of approximately 0.5-liter capacity, designed to insure complete isolation of the hydraulic pumping fluid from the gas mixture. If the gas were to become contaminated with hydrocarbons from the hydraulic fluid further contamination of the furnace and specimens would likely occur and perhaps cause erroneous results. Isolation is achieved by making the floating separator piston double-ended with Bridgman mushroom-type packings at either end. The wiping areas of the piston ends do not overlap.

The high-pressure portion of the system can be primed to 2000 bars through valve H by use of the separator. American Instrument Company 1/4-inch O. D. by 3/32-inch I. D. type 316 stainless steel tubing was used for the low-pressure

lines and Harwood 3/16-inch O. D. by 0.025-inch I. D. type 316 stainless steel tubing was used for the high-pressure lines. All low-pressure valves and connecting blocks are Aminco 30,000 psi type. A Harwood 200,000 psi valve was used in the high-pressure section.

The secondary gas-compression stage uses a 0.02-liter 15 to 1 Harwood intensifier driven by a 30,000 psi electric pump or a 40,000 psi Blackhawk hand pump.

Safety shielding of layers of 1/2 inch thick steel plate, 4 inches of sand and 1/2 inch of plywood was used for all components pressurized above 2000 bars.

The assembled pressure vessel and internal furnace is shown in cross-section in Figure 20 and the unassembled furnace is shown in Figure 21. All parts of the experimental vessel were machined from Bethlehem "Omega" tool steel and heat treated to a hardness of Rockwell C-52. The internal furnace was described in detail in the text.

Figure 17. Schematic drawing of the pressure system.

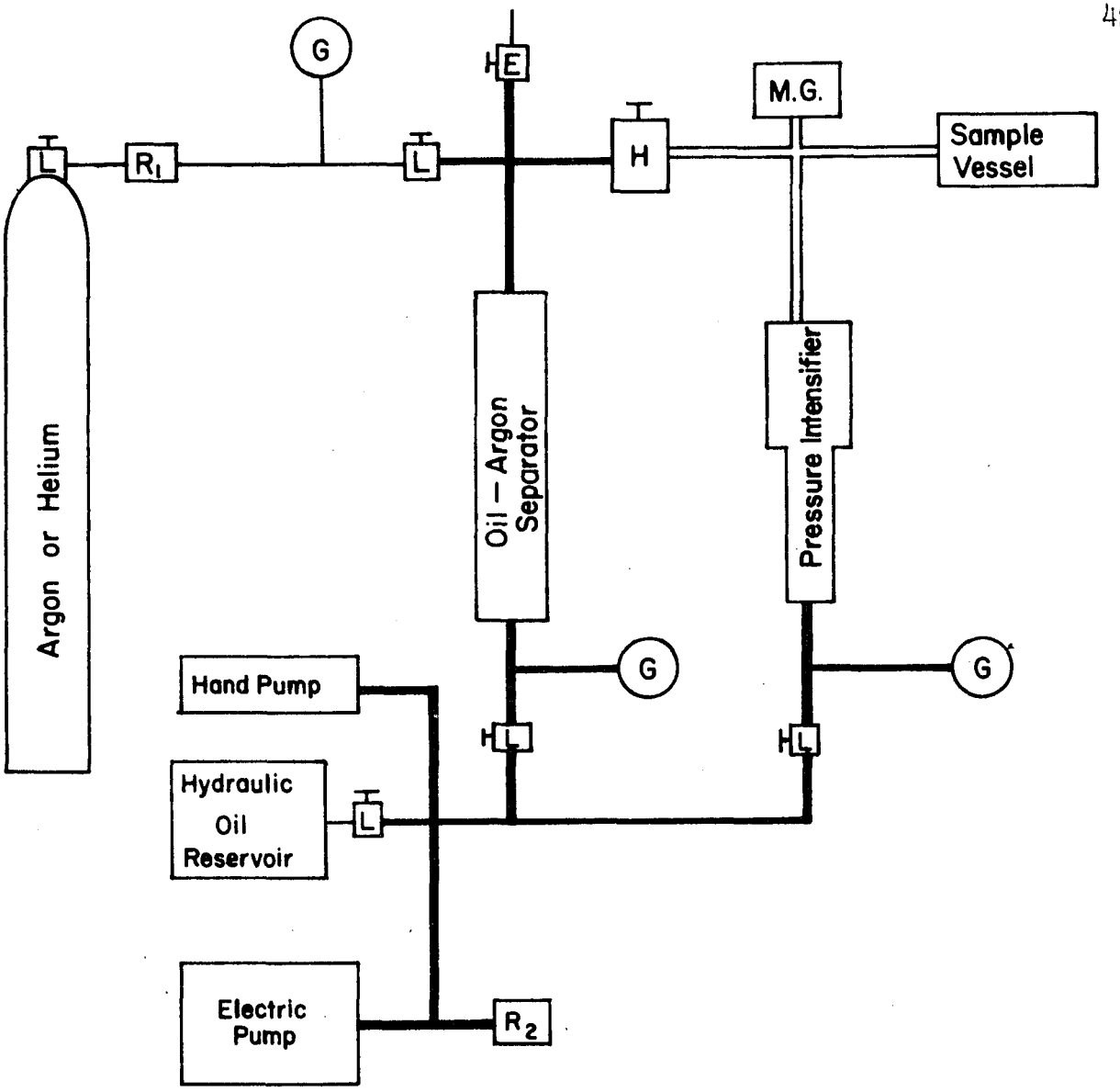
G
E
M.G.
Sample Vessel
L
R1
L
H
Argon or Helium
Oil – Argon Separator
Pressure Intensifier
G
G
Hand Pump
L
L
Hydraulic Oil Reservoir
L
Electric Pump
R2
G Bourdon Gauge
M.G. Manganin Gauge
L Low Pressure Valve
H High Pressure Valve
E Exhaust Valve
R1 Rupture Disk, 3500 PSI
R2 Rupture Disk, 35,000 PSI
4,000 PSI Tubing
1/4"-60,000 PSI Tubing
3/16"-200,000 PSI Tubing

Figure 17.

Figure 18. Pressure system controls.

Figure 19. Pressure system showing, from left to right, separator, small manganin gauge vessel, intensifier and horizontal experimental vessel housed within the safety barricade.

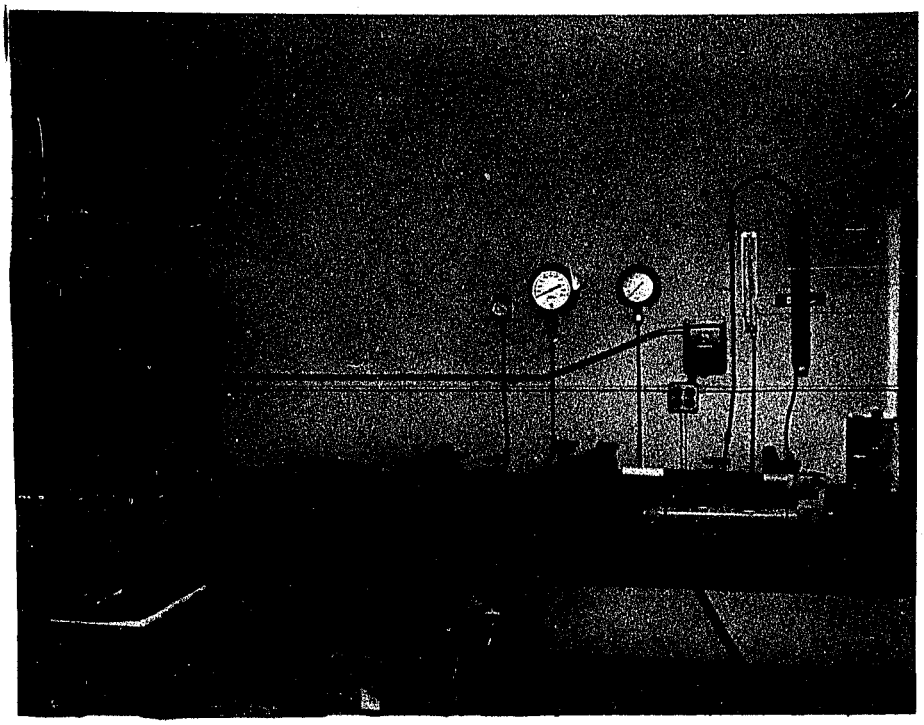

Figure 18

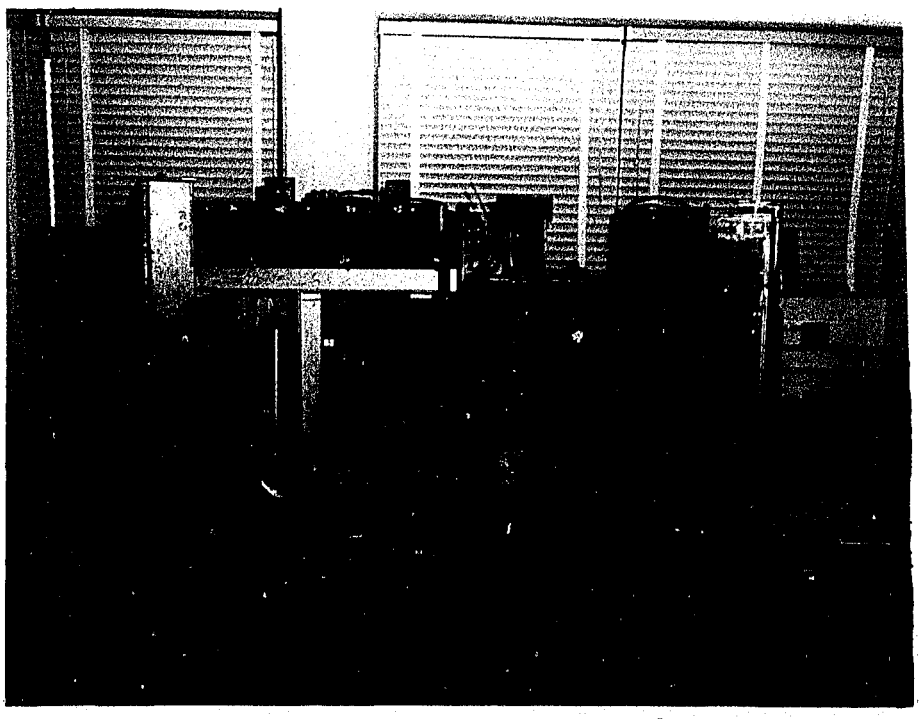

Figure 19

Figure 20. Cross-sectional drawing of the assembled experimental vessel and the high temperature internal furnace.

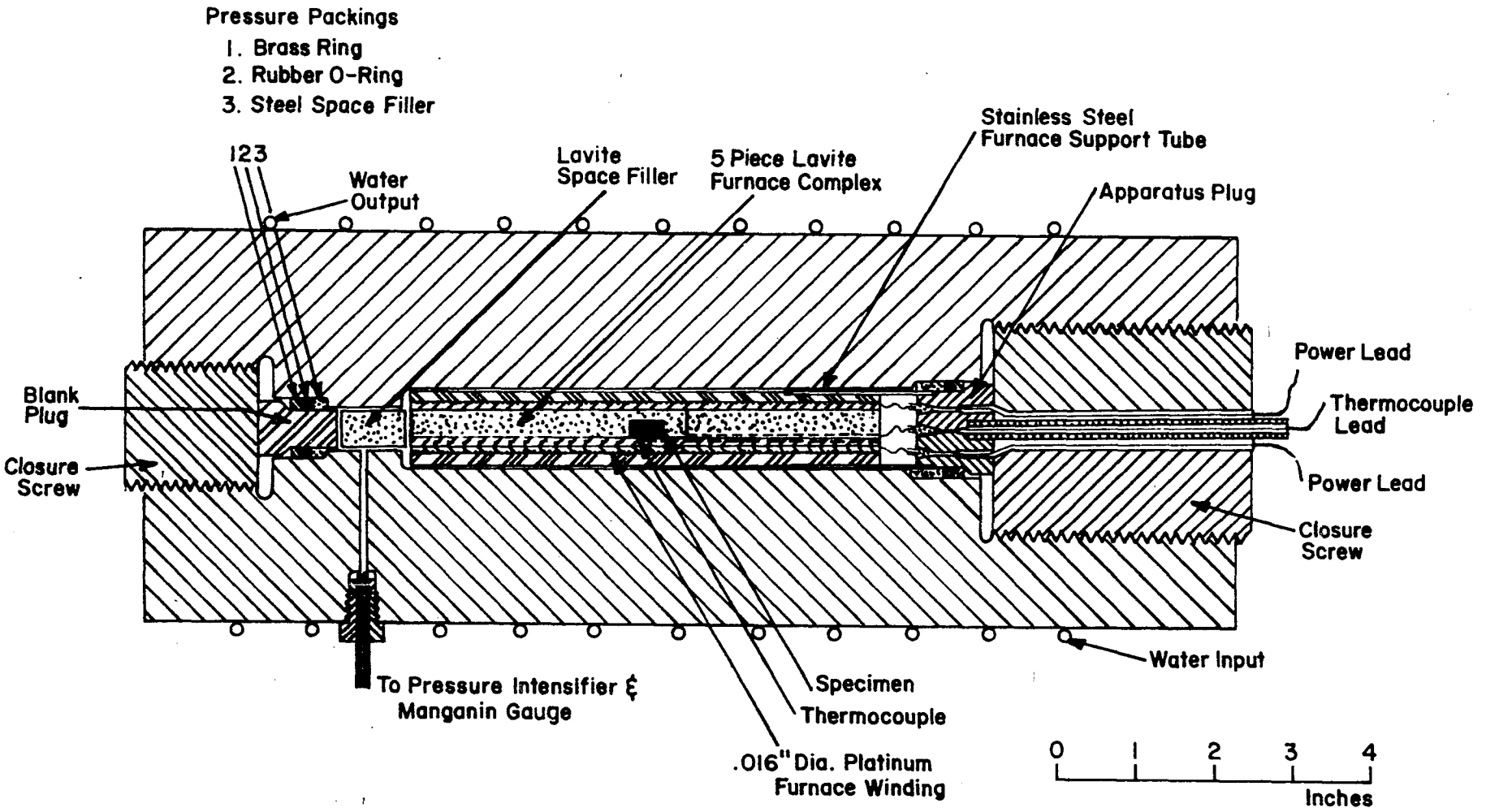
Pressure Packings
1. Brass Ring
2. Rubber O-Ring
3. Steel Space Filler
123
Water Output
Lavite Space Filler
5 Piece Lavite Furnace Complex
Stainless Steel Furnace Support Tube
Apparatus Plug
Power Lead
Thermocouple Lead
Power Lead
Closure Screw
Blank Plug
Closure Screw
Water Input
To Pressure Intensifier & Manganin Gauge
Specimen Thermocouple
.016" Dia. Platinum Furnace Winding
0 1 2 3 4
Inches

Figure 20.

Figure 21. Disassembled high temperature internal furnace showing all parts, specimen to be diffused, the experimental thermocouple configuration and the apparatus plug.

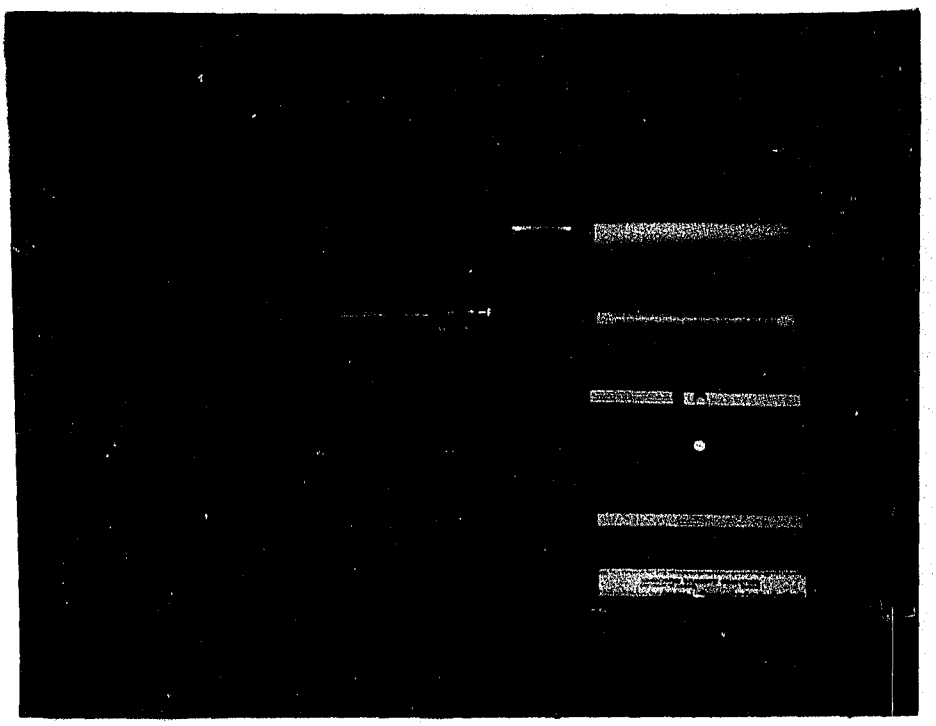

Figure 21

APPENDIX IV

Solution of the Diffusion Equation

Fick's first and second laws describe the diffusion of atoms in a homogeneous alloy system. If the diffusion is unidirectional, Fick's first law states:

$$J = -D \frac{dc}{dx}$$

where J is the flow of atoms across a unit area, c is the concentration of the tracer atom, x is the depth of penetration and D is the diffusion coefficient. In the radioactive tracer technique, the concentration c is assumed to be negligible and does not affect the composition of the alloy. As a result of these conditions, D is a constant independent of the depth of penetration x, and the surface concentration of the isotope c_o. When a continuity of mass and volume across the diffusion area are assumed, Fick's second law is:

$$\frac{dc}{dt} = D \frac{d^2c}{dx^2} .$$

When the boundary conditions of a semi-infinite crystal whose face is plated with an infinitely thin layer of diffusing atoms are imposed, the solution for the second law is:

$$c(x,t) = \frac{c(0,0)}{(\pi Dt)^{\frac{1}{2}}} \exp\ (-x^2/4Dt).$$

Substituting specific activity A for the concentration:

$$A(x,t) = \frac{A(0,0)}{(\pi Dt)^{\frac{1}{2}}} \exp\ (-x^2/4Dt).$$

Taking the natural logarithm of the equation above:

$$\ell n[A(x,t)] = \ell n[\frac{A(0,0)}{(\pi Dt)^{\frac{1}{2}}}] - (x^2/4Dt).$$

Differentiating with respect to x^2:

$$\frac{d[\ell n\ A(x,t)]}{d(x^2)} = \frac{-1}{4Dt}\ .$$

Transposing the above equation:

$$D = \frac{-1}{4t\ d(\ell nA)/d(x^2)}\ .$$

Therefore, if the common logarithm of the specific activity is plotted versus the square of the penetration distance, the diffusion coefficient may be determined from the relation,

$$D = \frac{-1}{(2.303)\ (4)\ (t)\ (slope)}\ .$$

Diffusion coefficients are related to temperature by an Arrhenius-type equation stated earlier in the text as,

$$D = D_o \exp(-H/RT).$$

Taking the natural logarithm of this equation:

$$\ell n\ D = \ell n\ D_o - H/RT.$$

Differentiating with respect to 1/T:

$$\frac{d(\ell n\ D)}{d(1/T)} = -H/R.$$

Transposing:

$$H = -R \frac{d(\ell n\ D)}{d(1/T)}.$$

The activation enthalpy, H, may be determined from the plot of common logarithm of diffusion coefficient versus the reciprocal of absolute temperature of the diffusion anneal by the relation,

$$H = (2.303)\ (R)\ (\text{slope}).$$